Experimental verification of sub-wavelength holographic lithigraphy (SWHL) concept

Borisov, M., Chelubeev, D., Chernik, V., Merkushov, L., Rakhovskiy, V., et al.

M. Borisov, D. Chelubeev, V. Chernik, L. Merkushov, V. Rakhovskiy, A. Shamaev, "Experimental verification of sub-wavelength holographic lithigraphy (SWHL) concept," Proc. SPIE 11324, Novel Patterning Technologies for Semiconductors, MEMS/NEMS and MOEMS 2020, 113241J (23 March 2020); doi: 10.1117/12.2552013

Event: SPIE Advanced Lithography, 2020, San Jose, California, United States

Experimental verification of sub-wavelength holographic lithography (SWHL) concept

M. Borisov, D. Chelubeev, V. Chernik, L. Merkushov, V. Rakhovskiy*, A. Shamaev
NANOTECH SWHL GmbH, Überlandstrasse 129, 8600 Dübendorf, Switzerland

ABSTRACT

Sub-Wavelength Holographic Lithography (SWHL) was introduced some years ago by Nanotech SWHL GmbH as a disruptive and promising method to replace projection photolithography. SWHL is based on principles of wave optics and uses a computer-generated hologram (CGH) as a photomask for both 2D and 3D imaging.

To proof the concept of SWHL first for sub-wavelength critical dimensions (CD) and then for non-flat imaging we designed two experimental optical set-ups. Both set-ups use commercially available 442nm He-Cd gas laser. The holographic masks were designed as a set of windows in an opaque chromium layer on a fused silica blank.

The imaging in SWHL does not require any projection optics. Thanks to this the optical system includes only the illuminator of the mask. The illuminator design is very simple, with just a few optical elements.

To demonstrate an image with sub-wavelength resolution, we use illumination with NA 0.53. For this NA we generated image with CD 250 nm that is 0.56 of the wavelength 442 nm.

To demonstrate 3D imaging capability the demonstration lab tool was developed. The tool provides the illumination of holographic mask with NA 0.24. The mask generated a multi-plane image with a depth of 100 μm and the image resolution of 2 μm.

We demonstrated both subwavelength and 3D holographic imaging in experiments and prove the concept of SWHL. All the experiments were made as computer simulations first. The comparison of the simulation and experimental results proved the reliability of our software.

Keywords: holographic lithography, holographic mask, computer generated hologram, digital holography, sub-wavelength lithography, 3D imaging

1. INTRODUCTION

The progress in the microminiaturisation of semiconductor devices leads to the fast growth of complexity and the cost of IC production. The complexity of high-end IC fabrication results from the principal limitations of UV projection photolithography, which is still the most used method of patterning of semiconductor wafers even after over 60 years of continuous scaling down of the IC feature size.

Projection masks for optical resolutions close to Rayleigh-Abbe limit 0.25λ/NA[1] are manufactured with the use of very complicated and expensive resolution enhancement techniques (RET), like OPC, Phase-**S**hift, OAI, SMO and ILT[2]. At the 193 nm wavelength the use of immersion combined with extremely complex projection lens, comprising tens of reflecting and refracting optical elements[3], with a large numerical aperture (NA=1.35)[4]. High NA and sophisticated illumination schemes allow to reach minimal-pitch 38.5 nm. This resolution requires masks and light sources with all aforementioned RETs employed.

Every defect appearing on a projection mask is translated directly into the image in photoresists, reduced by only four times. Consequently, a mask leaving mask shop or cleaning/repair step should not have any defect with the size more than 40% of the lithographic CD**.** This is indeed a very tough requirement. The most complicated phase-shift masks[5] suffers from defects most of all. These masks have a phase-shifting layers of transparent dielectric materials. Such layers are not tolerant to ion etching that is used to clean the masks and can be critically damaged after several cleaning attempts. This limits the number of possible mask cleaning cycles. Therefore, the cost of masks production and repairing becomes a significant part of the total cost of lithographic stage of IC production.

*rakhvi@nanotech-swhl.com; phone +41 79 583 19 57; nanotech-swhl.com

Novel Patterning Technologies for Semiconductors, MEMS/NEMS and MOEMS 2020,
edited by Martha I. Sanchez, Eric M. Panning, Proc. of SPIE Vol. 11324, 113241J
 · doi: 10.1117/12.2552013

The high complexity of lithography equipment and mask structure caused a huge growth of lithography equipment and mask costs, especially for high-end applications.

The development of microelectronics has led to the emergence and continuous expansion of the scope of applications of 3D components in low-end market, which include MEMS, MOEMS, microchannels, etc. Projection photolithography used to create 3D patterns faces the trade-off between resolution ($R \sim NA^{-1}$) and depth of focus ($Z \sim NA^{-2}$). Flat projection mask can only generate a single flat image; hence it is impossible to simultaneously create images in multiple planes placed apart by distances significantly larger than the depth of focus of the projection system.

Meeting the demands of low-end market requires the development of new methods of 3D patterns imaging, which is quite difficult to implement using projection lithography. The binary optics techniques have disadvantages such as multiple exposures, subsequent complex and precise alignment process, long production time and high cost. The gray-scale mask technique requires a gray-scale mask, which is difficult to design and expensive to manufacture.

Many of the difficulties noted above are largely related to the necessity of eliminating distortions of image elements caused by diffraction on corresponding topological elements of a projection mask. These issues arise since the projection imaging approach has been originally based on geometrical optics and still inherits overall direction to struggle against the diffraction effects. The approach we propose is based on the holography and uses the wave nature of light instead of overcome it.

There were a few attempts to use holographic masks in photolithography. The experimental results for Fresnel holograms[6] and total internal reflection holograms[7,8] were reported. These holograms were optically recorded and the methods are limited by a properties of material object.

We believe that all the above-mentioned fundamental limitations of projection lithography can be successfully got over by the transition from projection imaging approach to holographic one, which is used in Sub-Wavelength Holographic Lithography (SWHL)[9,10,11]. SWHL is based on principles of wave optics with high coherent light and uses diffraction to create images both in 2D and 3D. Such an approach offers a much simpler and less expensive lithographic technology, both for high-end and low-end (MEMS, MOEMS, etc.) applications.

In this paper we present the experimental proof-of-concept of SWHL for both subwavelength and 3D holographic imaging.

2. EXPERIMENTAL TOOLS AND METHODOLOGY

2.1 First experimental set-up for verification of sub-wavelength capabilities of SWHL

To proof the concept of SWHL to pattern test images with subwavelength CD the experimental optical set-up was designed and assembled (Fig. 1, 2).

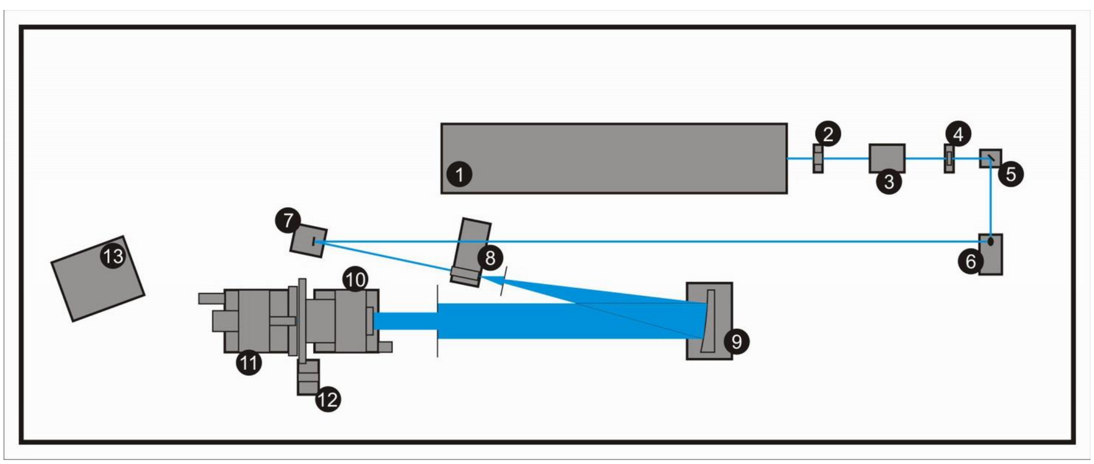

Figure 1. Schematic of the experimental set-up for sub-wavelength imaging demonstration.

The set-up used He-Cd laser 1 with 442 nm wavelength. The light was controlled by the shutter 2, the attenuator 3, the half-wave plate 4 and directed by the mirrors 5-7 to the beam expander 8-9. The unit 10 included the illumination lens and the holographic mask. The unit 11 included wafer chuck and digital microscope for real time image inspection. The field stop unit 12 was used to specify the exposed area on the wafer. The illumination lens generates convergent beam that illuminated the holographic mask. The numerical aperture (NA) of the beam was 0.53.

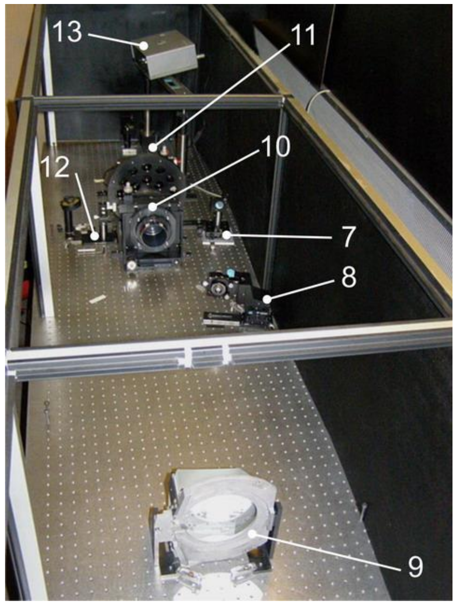

Figure 2. Photo of the experimental set-up for sub-wavelength imaging demonstration (laser is not shown).

For the first experimental tool we designed the test pattern with CD = 250 nm and 350 nm (Fig. 3). Compared to the working wavelength 442 nm these CD can be considered as a reliable proof of subwavelength imaging with SWHL. This test pattern included some sets of periodic lines to provide a comparison of imaging for the elements of different directions.

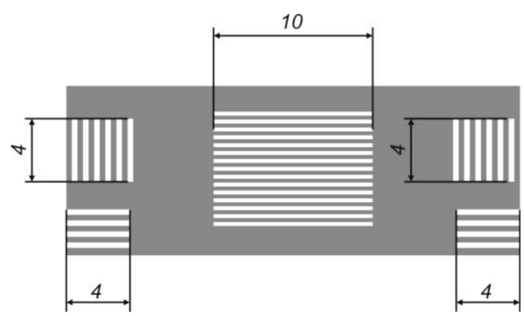

Figure 3. Test image design. All the dimensions are in μm. CD = 0.25 μm

The holographic mask (Fig. 4) was calculated by using the specific software that we developed for SWHL.

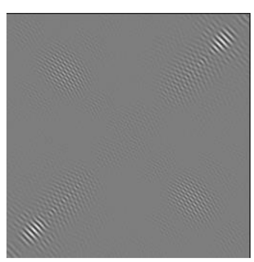

Figure 4. Holographic mask (top view of the working area).

The mask consisted of a set of elements (windows in opaque screen) that were distributed by a square grid of 21.12 μm. The size of the elements was in the range of 0.33 μm to 20.79 μm. The mask was manufactured by a common chromium-on-quartz technology. The mask working area was 12 mm ×12 mm and the image was generated at the distance of 13.4 mm from the mask.

For lithography patterning we used 150 mm silicon wafers covered with photoresist layer. The photoresist was required to provide a reasonable contrast at 442 nm exposure for 250 nm resolution. Because such a photoresist was not available at the time of the experiments, we used an h-line (408 nm) photoresist diluted for 150 nm thickness of the wafer coating. Anti-reflection coatings (ARC) were not used.

2.2 Advanced experimental tool for verification of 3D capabilities of SWHL

To proof the concept of SWHL to pattern 3D (non-flat) images the experimental optical tool was designed and assembled (Fig. 5, 6).

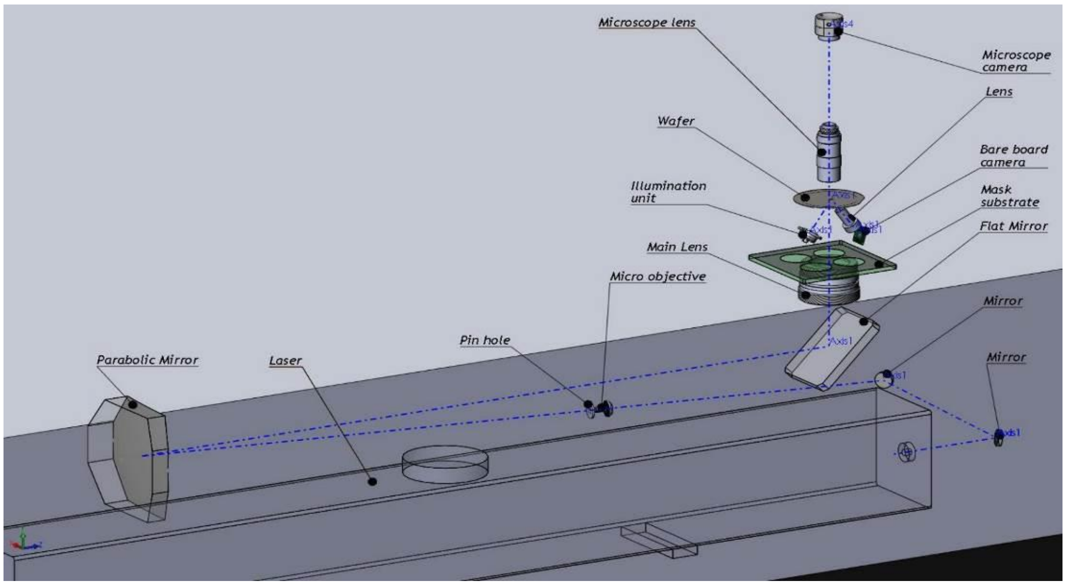

Figure 5. Schematic of the experimental tool for 3D imaging demonstration.

Figure 6. Photo of the experimental tool for 3D imaging demonstration.

The schematic of this experimental tool was similar to the first one (see Fig. 1). The main difference is that the direction of illumination and imaging beam was vertical as it is usual for photolithography tools. The tool used He-Cd laser with 442 nm wavelength. The light was directed by the mirrors to the beam expander based on a parabolic mirror. The holographic mask was illuminated by the main lens with NA 0.24.

For 3D tests we designed some test patterns with CD = 1 μm and CD = 2 μm (Fig. 6). Compared to the working wavelength 442 nm and NA 0.24, this resolution level can be considered as a reasonable resolution for imaging with

SWHL. The design of the test pattern is shown in Fig. 7. The pattern covered the non-flat surface with periodic cavities. The cavities were 350 μm × 350 μm in plane and had 100 μm depth.

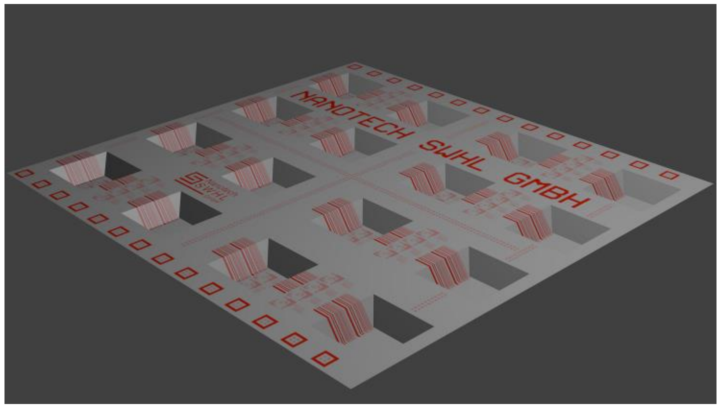

Figure 7. Design of the test pattern for 3D (non-flat) imaging demonstration.

The holographic mask (Fig. 8, 9) was calculated by using the software that we developed for SWHL.

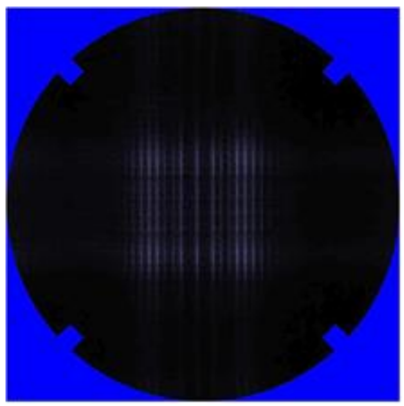

Figure 8. Holographic mask for 3D imaging (top view of the working area).

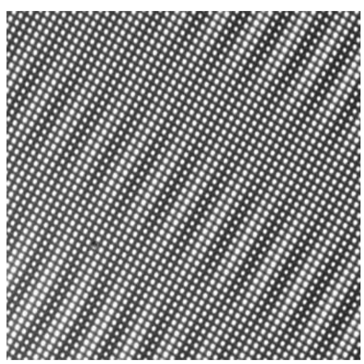

Figure 9. Microscopic photo of holographic mask for 3D imaging.

The mask consisted of a set of elements (windows in opaque screen) that were distributed by a square grid of 2 μm. The size of the elements was in the range of 0.75 μm to 1.9 μm. The mask was manufactured by a chromium-on-quartz technology. The mask working area was 44 mm diameter and the image was generated at the distance of 88.3 mm from the mask.

For lithography patterning we used 100 mm silicon wafers covered with photoresist layer. For first resolution tests we used i-line AZ 1505 photoresist and that can provide a contrast at 442 nm exposure for 1 μm resolution. We covered flat wafers with 400 nm films of the photoresist. Because that photoresist is not applicable for spray coating that is required for the wafers with a deep topography, we then used i-line AZ 4999 photoresist from Microchemicals. Spay coating allowed us to get 1.6 µm resist film with reasonable thickness variations. For resist development we used the AZ400K solution at 1:4 dilution. Anti-reflection coatings were not used.

3. EXPERIMENTAL RESULTS

3.1 Sub-wavelength patterning by using the first experimental set-up

The research of the subwavelength imaging we start with a computer simulation of the holographic image (Fig. 10) by using our software. The simulation result demonstrated a reasonable quality of the calculated holographic mask.

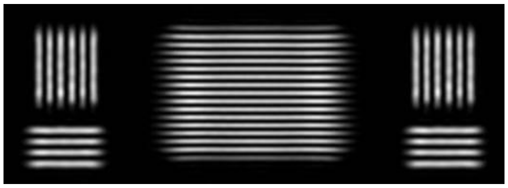

Figure 10. Computer simulation of holographic image.

Then we used the holographic mask for imaging in the experimental set-up (see Fig. 1, 2). The holographic image was captured by the CCD camera of the digital macroscope (Fig. 11). Then, a wafer with photoresist was patterned by the holographic image (Fig. 12).

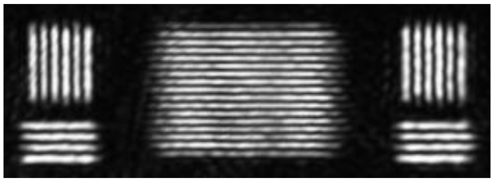

Figure 11. Holographic image captured by a CCD camera.

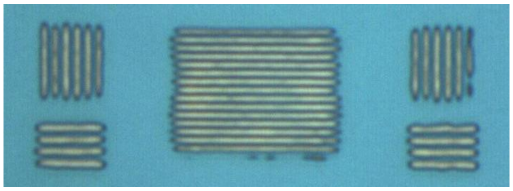

Figure 12. Pattern in photoresist.

The pattern in photoresist was inspected and measured by SEM (Fig. 13). The inspection demonstrated the resulting half-pitch resolution of about 250 nm that is 0.56 of the wavelength 442 nm.

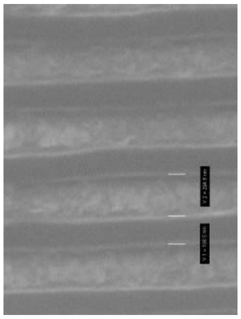

Figure 13. SEM image of the patterned photoresist.

3.2 Patterning of non-flat wafers by using the advanced experimental tool

We started our experiments with tests of imaging resolution. These tests were made with flat wafers. The results of imaging are shown in Table 1.

Table 1. Resolution test results for computer simulation and experimental imaging (figures ref. to linewidth, μm).

Pattern design	Aerial image (comp. simulation)	Photoresist (comp. simulation)	Aerial image (CMOS-camera)	Photoresist (microscope)
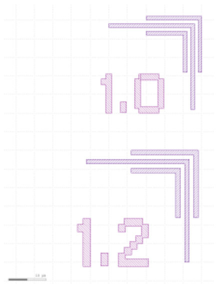		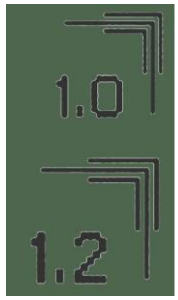	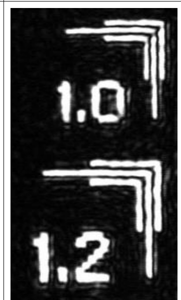	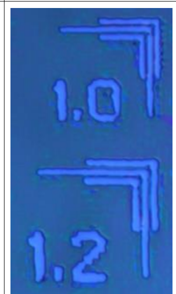
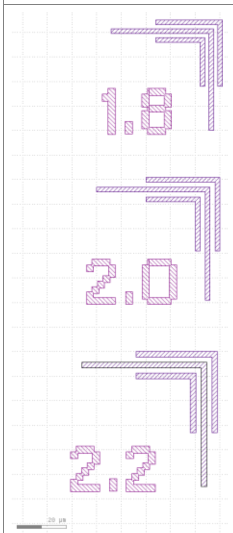			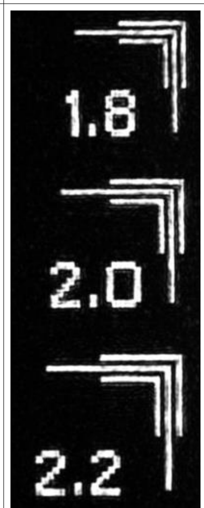	
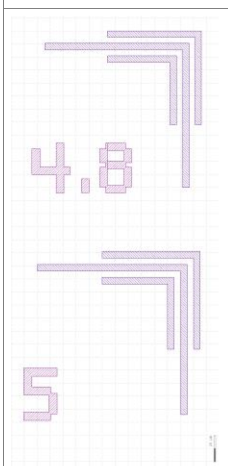			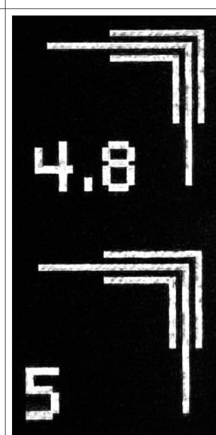	

The experimental research of non-flat imaging we started with image resolution 1 µm. The results of imaging are shown in Table 2.

Table 2. Non-flat imaging results for computer simulation and experimental imaging.

	Pattern design (min. line width 1 µm)	**Aerial image (CMOS-camera)**	**Photoresist (comp. simulation)**
Top plane	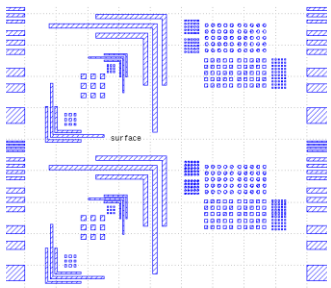	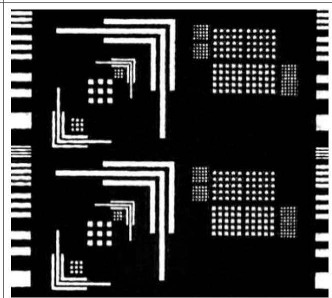	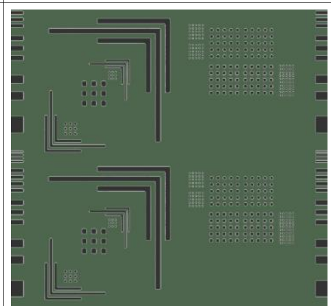
Bottom plane	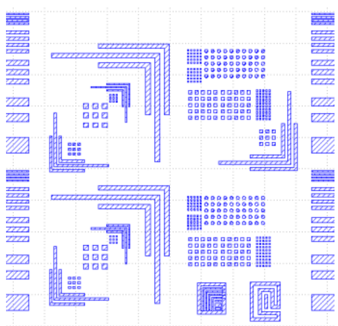	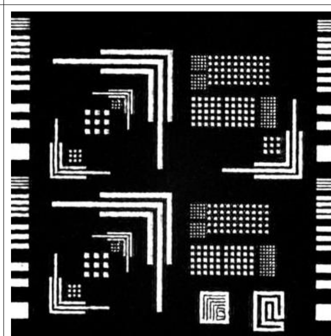	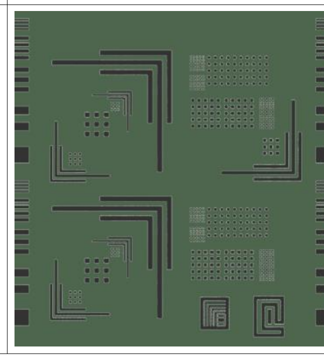

For patterning of structured (non-flat) wafers with 100 µm depth topography we used holographic images with resolution 2 µm. The patterning results are shown in Fig. 14, 15.

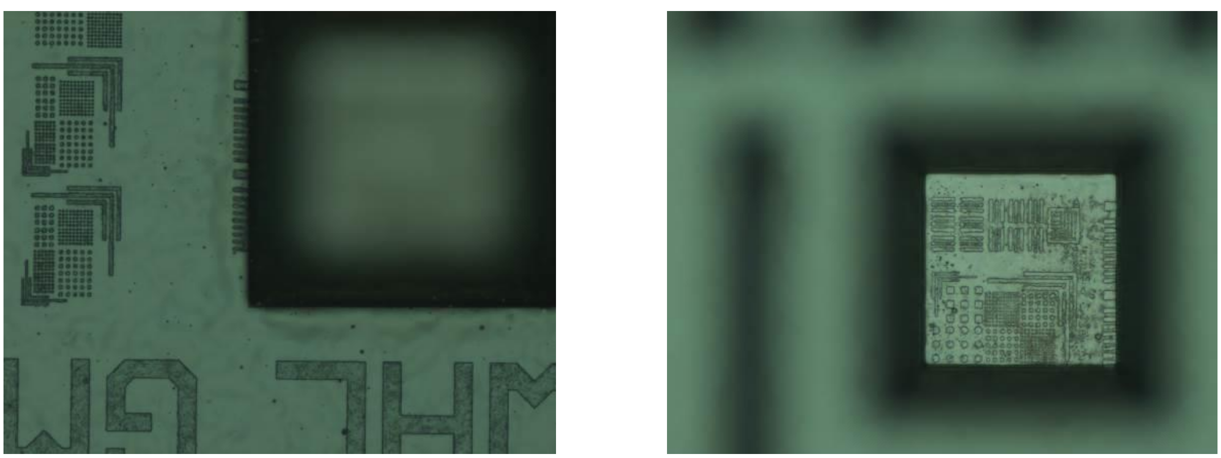

a b

Figure 14. Pattern in photoresist on the structured wafer: a – top of the wafer surface; b – bottom of the wafer surface (top to bottom depth 100 µm).

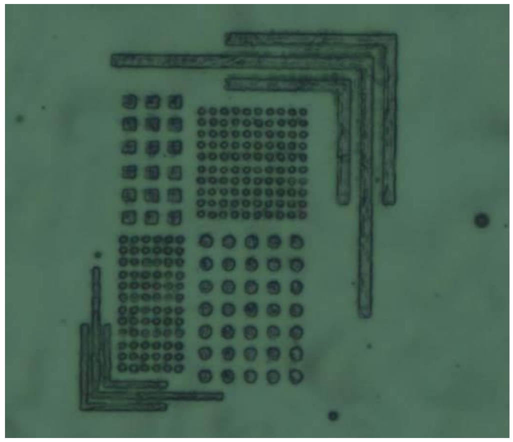

Figure 15. Pattern in photoresist. Min. line width 2 μm.

4. DISCUSSION

The patterns that we made with the first experimental set-up definitely confirms the capability of SWHL to generate patterns with sub-wavelength resolution. The image elements are completely resolved and are in a good correspondence with computer simulations.

Nevertheless, the pattern in photoresist demonstrates suffers from distortions of different kinds. The main reason of this is the non-optimal exposure, because the resist has a very low contrast at 442 nm wavelength. The other reason is a non-optimal mask calculation. This optimization requires to develop a correct photoresist model that can be taken into account during the mask calculation. Further, we understand that the depth of focus of the images are not big enough and this is also a severe reason of the image quality degradation. We will enhance our software to take into account the depth of focus optimization.

In this work the image area was very small but we had no goal to get large patterns and reach small ratios of the mask-to-image size. In our subsequent work we used special techniques during a mask synthesis in order to significantly reduce this ratio.

The results of the experiments with the advanced experimental tool demonstrates the capability of SWHL to generate patterns on non-flat surfaces. We get patterns on the wafer with a topography depth of 100 μm with imaging depth of focus of about 4 μm and resolution of 2 μm. These patterns were exposed with one mask at one exposure. Again, we demonstrated a very good correspondence of the experimental images and the computer simulations.

The inspection of the patterns demonstrates imperfections in the resist development. At the same time the patterns on the bottom plane of the cavities suffer from additional light noise. The main reason of it is a strong reflection from the substrate. Because of its high coherence, the light interferes and generates unwanted distribution of the light intensity. We expect that proper anti-reflection coatings can be a solution. Also, we suppose that changing of the working wavelength to i-line range can help because of more correct resist response.

5. CONCLUSION

In this work we confirmed a concept of generation images with elements up to the subwavelength resolution by SWHL method. The half-pitch resolution of 250 nm at 442 nm wavelength and NA 0.56 reliably demonstrates lithography CD on the subwavelength level.

We also verified a capability to generate 3D images and to pattern non-flat wafers from one mask and single exposure.

Very good correspondence of experimental results and computer simulations are demonstrated. We confirmed the validity of theoretical assumptions, the performance of mathematical models, algorithms and software for calculating the holographic masks, the practical applicability of the proposed technical solutions.

Further we are going to work on the enhancement of the holographic lithography process to increase quality of the patterns. We are also planning to demonstrate 3D patterning in thick photoresist by means of holographic grey-scale lithography.

REFERENCES

[1] Mack, C. A., [Fundamental Principles of Optical Lithography: The Science of Microfabrication] 101.1., John Wiley & Sons, 417 (2007)

[2] Mack, C. A., [Fundamental Principles of Optical Lithography: The Science of Microfabrication] 10.2.2., John Wiley & Sons, 411-457 (2007)

[3] Xiangung Luo [Engeneering Optics 2.0], ISBN 978-981-13-5755-8 (eBook), Springer Nature Singapore Pte Ltd., 294-295 (2019)

[4] ASML Scaner 2000i https://www.anandtech.com/print/13143/asml-ships-twinscan-nxt2000i-scanner-7nm-5nm

[5] Harry J. Levinson, H. J., [Principles of Lithography], Bellingham, USA: SPIE Press, 330-334 (2010).

[6] Beesley M. J., Foster H., Hambleton K. G., “Holographic projection of microcircuit patterns,” Electronic Letters 4, 49-50 (1968)

[7] Chen T. R., “Limitations of submicron holographic lithography,” Proc. SPIE 2337, 138-142 (1994)

[8] Barge M. at al., “120-nm lithography using off-axis TIR holography and 364 nm exposure wavelength,” Micro. Eng. 57-58, 59 (2001)

[9] Borisov M. V., Chelyubeev D. A., Chernik V. V., Gavrikov A. A., Knyazkov D. Yu., Mikheev P. A., Rakhovskiy V. I., Shamaev A. S., “Analysis of an Effect of Perturbations in SWHM and Illuminating Optical SchemeParameters on an Aerial Image,” Proc. of Advanced Semiconductor Manufacturing Conference, 23rd Annual SEMI, 165-169 (2012)

[10] Borisov M. V., Chelyubeev D. A., Chernik V. V., Gavrikov A. A., Knyazkov D. Yu., Mikheev P. A., Rakhovskiy V. I., Shamaev A. S., “Phase-shift at subwavelength holographic lithography (SWHL),” Proc. SPIE 8352, 28th European Mask and Lithography Conference, 83520P (2012)

[11] Borisov M. V., Chelyubeev D. A., Chernik V. V., Mikheev P. A., Rakhovskiy V. I., Shamaev A. S., “Experimental verification of sub-wavelength holographic lithography physical concept for single exposure fabrication of complex structures on planar and nonplanar surfaces,” Proc. SPIE 10446, 33rd European Mask and Lithography Conference, 104460X (2017)